

Article

Towards the Efficient Way of Asphalt Regeneration by Applying Heating and Mechanical Processing

Vytautas Bucinskas , Andrius Dzedzickis * , Mantas Makulavicius, Nikolaj Sesok and Inga Morkvenaite-Vilkonciene

Department of Mechatronics, Robotics and Digital Manufacturing, Faculty of Mechanics, Vilnius Gediminas Technical University, 03224 Vilnius, Lithuania

* Correspondence: andrius.dzedzickis@vilniustech.lt

Abstract: Asphalt layers renovation includes heating, mechanical processing, and the removal of the layer. Implementation of an alternative method—regenerating the upper asphalt layer, saves the operation time and energy. Common regeneration technologies consume a significant amount of energy and pollute the air during operation. This research aimed to investigate the improvement of the asphalt layers regeneration process when heating is applied together with mechanical processing. This methodology enables safe energy in the process of asphalt regeneration in terms of heating agent and mechanical processing. The distribution of the asphalt temperature in its cross-section with and without mechanical processing was evaluated experimentally and theoretically using a mathematical model. Experiments were performed in the temperature range from 250 to 450 °C. Mechanical loading was applied by the pressure force of 4500 N. Using mechanical loading together with heating, the best heat transfer into a deeper layer was found when the heating temperature of the asphalt was 250 °C. The asphalt simulation model showed that deeper asphalt layers require more time for the temperature to reach the limit values.

Keywords: asphalt; heating; regeneration; heat transfer; FEM modeling



Citation: Bucinskas, V.; Dzedzickis, A.; Makulavicius, M.; Sesok, N.; Morkvenaite-Vilkonciene, I. Towards the Efficient Way of Asphalt Regeneration by Applying Heating and Mechanical Processing. *Coatings* **2022**, *12*, 1785. <https://doi.org/10.3390/coatings12111785>

Academic Editors: Tian-Feng Yuan and Sharareh Shirzad

Received: 24 October 2022

Accepted: 18 November 2022

Published: 21 November 2022

Publisher's Note: MDPI stays neutral with regard to jurisdictional claims in published maps and institutional affiliations.



Copyright: © 2022 by the authors. Licensee MDPI, Basel, Switzerland. This article is an open access article distributed under the terms and conditions of the Creative Commons Attribution (CC BY) license (<https://creativecommons.org/licenses/by/4.0/>).

1. Introduction

The increasing quantities and types of waste, the lack of landfills, and the scarcity of natural resources show that innovative ways of recycling and reusing waste are needed. If not properly recycled, these large amounts of waste are landfilled every year, and natural resources are quickly depleted due to the high demand for raw materials. Modern road construction technologies ensure surface durability, comfort, and consumer safety while being environmentally friendly and affordable. The road quality depends on the asphalt properties that can be affected by its composition, exploitation time, climate conditions, and traffic intensity [1,2]. For example, at low temperatures, the stress–strain behavior of viscoelastic materials (such as asphalt and other bituminous-based mixtures) depends on the stresses, the loading conditions, and on other important related factors. On the other hand, at high temperatures, due to the energy dissipating by the maltenes during the loading cycle and ultraviolet (UV) light, the viscosity of the bitumen is increased, which becomes more hard and brittle, increasing the stiffness of asphalt [3]. Upper asphalt layers are affected by UV (UV aging) as well by destroying the molecular structure of asphalt binders [4–6]. Defected asphalt coating requires restoring its structure and properties to the desired level.

In the asphalt recycling industry, there are five common asphalt pavement recycling technologies: hot in-place recycling (HIR), hot central-plant recycling (HCPR), cold in-place recycling (CIR), cold central-plant recycling (CCPR), and full-depth reclamation (FDR) [7]. The construction technology of HIR is considered to be one of the most effective approaches against others [8]. It is easy to control, it can be used in a wide range of applications, e.g., to

rehabilitate deteriorated asphalt pavement or to improve the reclaimed asphalt pavement (RAP) performance [9–11]. The heating of the asphalt upper layer can be applied in low temperatures without a negative effect on the environment. RAP content is relatively low at generally 10–40%, recycling depth is relatively low at 40 mm [7]. HIR saves 5% of the cost and reduces overall environmental impacts by 16% compared with milling and filling (M&F), while M&F energy consumption is 7% lower than HIR [12]. The production of 100% recycled hot mix concrete can be achieved using multiple technologies [13]. HIR is deemed an environmentally friendly maintenance measure of the asphalt pavement due to its complete recycling of aged asphalt mixture. The environmental burden when hot in-place recycling of asphalt pavement was simulated in [14]. The authors defined that with the same paving mass, the emissions of the remixing method were greater than the repaving method by 19–21%. With the same paving length, the emissions of the remixing method were less than those of the repaving method by 23–26%. The heating effects of asphalt pavement during hot in-place recycling using the discrete element method (DEM) are investigated in [15]. Researchers determined that the one-way continuous heating method leads to asynchronously reaching the highest temperature in lower layers like the upper part of the heated pavement layer. Asphalt concrete is a mixture that consists of three main phases: aggregate, binder, and air voids [16]. The layer of cracked/defected asphalt can be removed, processed (e.g., milled), and reused [17,18]. RAP materials can be used for the construction and rehabilitation of road pavements [19].

Our research includes the improvement of the asphalt regeneration process when the heating process is combined with mechanical treatment. This research investigates heat penetration into the required depth from asphalt to layer surface, especially in the situation, when the heat is applied from the top and therefore the direction of heat propagation is opposite to natural convection. The standard asphalt rehabilitation process covers an asphalt layer depth of 40 mm [7], consequently experimental research and finite element method (FEM) model focused on this depth. The heating process during the asphalt rehabilitation process is limited by the chemical decaying of bitumen in the high-temperature area, the softening degree of the bottom of the processed layer, and adequate heating duration.

The aim of this paper is the dynamics evaluation of the asphalt layer heating process, using the traditional heating process, and heating combined with mechanical treatment. Mechanical treatment will: (a) close gaps between aggregate particles and thus improve heat propagation; (b) darken the color of the asphalt layer and increase absorption of heat, radiated from the heating surface; (c) increase asphalt top surface area.

2. Modelling and Simulation

2.1. Asphalt Material Fragment Model

The process of mechanical treatment during asphalt remix is based on the conception of modifying the thermal conductivity of the asphalt layer. The thermal conductivity of the asphalt layer depends on the properties of its compounds. The typical value of various asphalt mixtures approximately varies from 0.7 W·m/K to 1.7 W·m/K [20,21]. This parameter is limited by the properties of used asphalt bitumen (binder) since the thermal conductivity of bitumen (0.17–0.2 W·m/K) is much lower than the conductivity of aggregate (1.5–2.2 W·m/K) [20]. Assuming that by applying mechanical force, it is possible to minimize the distances between aggregate particles in the asphalt mixture. When normal force was applied to the heated asphalt layer, the amount of air voids in the bitumen was minimized, and the thermal conductivity of the deformed asphalt layer will increase. Such a treatment will allow minimizing the energy and time consumption required for the asphalt layer rehabilitation.

For an illustration of this method, we used special asphalt material fragment modeling using FEM. This model is used to define the change of heat transfer through the enveloping layer between granite particles in the case of mechanical treatment under heating. This case assumes a mechanical force applied to the deteriorated layer of the asphalt to create better heat transfer conditions. The developed model (Figure 1a) consists of two granite particles

(10 and 12 mm in diameter) separated by a 3 mm thick layer containing hard particles and treated as a unified layer in the FEM model (Table 1). A bitumen layer of 3 mm with small hard includes detected in the area of testing. The bitumen layer is modeled as a visco-plastic material that can deform irreversibly at certain conditions, for example, when temperatures approach the melting point. Since the elastic modulus of bitumen depends on the temperature, the value of elastic modulus under 40 °C, was selected [22]. This is the minimum temperature required for asphalt rehabilitation at the site.

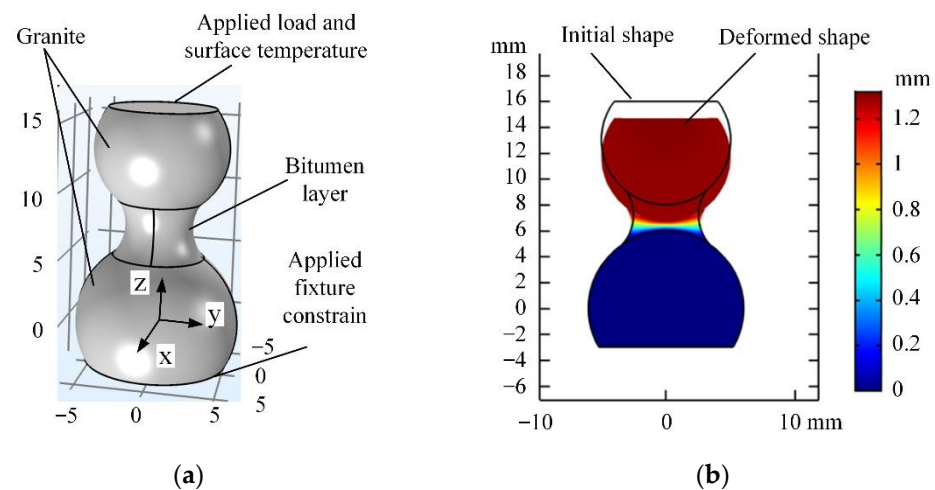


Figure 1. Model of asphalt material fragment: (a) boundary conditions and (b) displacement after applying load.

Table 1. Main properties of materials used in the simulation.

Material Parameter	Granite	Bitumen
Density, kg/m ³	2600	1016
Young's modulus, Pa	60×10^9	5×10^9
Poisson's ratio	0.25	0.45
Heat capacity at constant pressure, J/(kg·K)	850	2093
Heat transfer coefficient, W/(m ² ·K)	1.781	0.17

Figure 1b shows displacement results when the upper particle is loaded by the pressure of 2.5 MN/m². The black contour represents the initial shape, while a colored silhouette shows the deformed shape. The bitumen layer is compressed by 1.2 mm, which corresponds to a decrease in layer thickness by 40%.

After assessing the nature and magnitude of the deformation, the second step was to evaluate the impact of deformation on the heat transfer characteristics. Therefore, we determined and compared heat transfer speed in both the deformed and original models. The comparison was performed simulating the case where the environmental temperature is 17 °C and the temperature of the upper granite particle upper surface (Figure 1a) is 100 °C. Obtained results (Figure 2) show temperature change with respect to time in the center point of the lower part (Figure 1a $x = 0$; $y = 0$, $z = 0$).

It is seen, the mechanical impact had a positive effect on heat transfer properties, after 30 s of heating the temperature in the lower part is 1.5 °C higher compared with the same case in the undeformed state. M results show that mechanical deformation has two significant impacts affecting heat transmission properties: it reduces the thickness of the bitumen layer; increases the surface area of contact points between separate particles in the asphalt mixture. This modeling proves the functionality of the proposed idea, that mechanical treatment of the heated asphalt layer can increase the efficiency of the regeneration process, and that has been confirmed by the further presented results of the theoretical and experimental research.

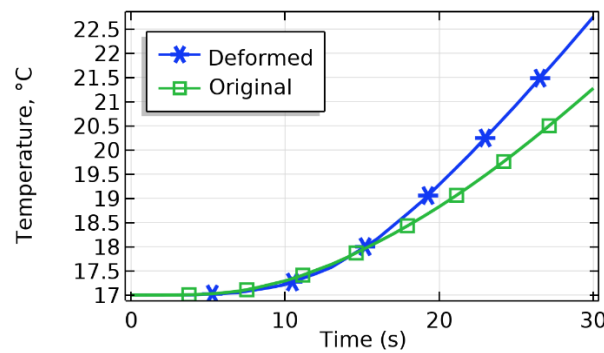


Figure 2. Comparison of heat transfer speed in original and deformed conditions.

2.2. Asphalt Layers Model

Due to the use of the co-sintering technique, the effective thermal resistance of porous asphalt media is very high and satisfies the heat transfer demand of many engineering applications. Natural convection in an enclosure filled with porous media or free convection on a surface sintered with metal foams has been studied to a certain extent [23].

According to [24–27], the total stored energy E of the system could be determined as the sum of internal energy, kinetic energy, and potential energy:

$$E = U + KE + PE, \tag{1}$$

where U—internal energy of the system; KE—kinetic energy; PE—potential energy.

The amount of the stored total thermal energy could be determined by defining a control volume and evaluating input and output energy transport caused by convection and diffusion. The work done by external forces at the surface of the control volume, including viscous forces, gravity force, and the heat source according to [24,25] can be modeled by:

$$\frac{\partial(\rho e)}{\partial t} + \text{div}(\rho V e) = -\text{div}(j_q) + \text{div}(\tau V) + \rho(\vec{g} V) + \dot{Q}, \tag{2}$$

where e is energy per unit mass ($e = E/m = u + 0.5 |V|^2 + gx_i$) and ρe is the energy per unit volume. After rearranging the mathematical expressions, the conservation equation for the total energy can be expressed in terms of enthalpy (h), as shown [24,25]:

$$\frac{\partial(\rho h)}{\partial t} + \text{div}(\rho V h) = -\text{div}(j_q) + \dot{Q}_s, \tag{3}$$

where j_q is a diffusion term, which comprises heat transfer by conduction and enthalpy transport due to moisture transfer, and Q_s is a heat source (or sink).

Expressing the transient convection and diffusion terms using mixture enthalpy (i.e., moisture, air, and solid matrix), and subsequent simplification of Equation (2) yields the mathematical model for transient heat transfer through porous media as in [24,25]:

$$\rho_m C_{p_{\text{eff}}} \frac{\partial T}{\partial t} + \rho_a (C_{p_a} + \omega C_{p_v}) \text{div}(VT) + \text{div}(-\lambda_{\text{eff}} \nabla T) = \dot{m}_c h_{fg} + \dot{m}_c T (C_p - C_{p_{v1}}) + \dot{Q}_s, \tag{4}$$

where $C_{p_{\text{eff}}}$ is the effective specific heat capacity, λ_{eff} is the thermal conductivity (which takes moisture effect into account), $\dot{m}_c = \text{div}\left(\delta_v \frac{\partial p_v}{\partial x_i}\right) - \rho_a \text{div}(V\omega)$ is the amount of moisture condensation/evaporation in kg/s.

Provided mathematical model, based on the defined heat transfer through porous media equation, was solved using “Comsol Multiphysics” software for FEM simulation. Later, simulated data are compared with experimental data.

The model was built and solved by the “Comsol Multiphysics” program, using geometry shown in Figure 3. The heating plate was placed on the asphalt layer with the properties

of the same material (Table 2) for both parts. The physics “Heat Transfer in Solids” was chosen with convective heat flux, thermal contact at the junction, and surface-to-ambient radiation. Coefficients are provided in Table 2. Experimental data have been compared to the model in Figure 4.

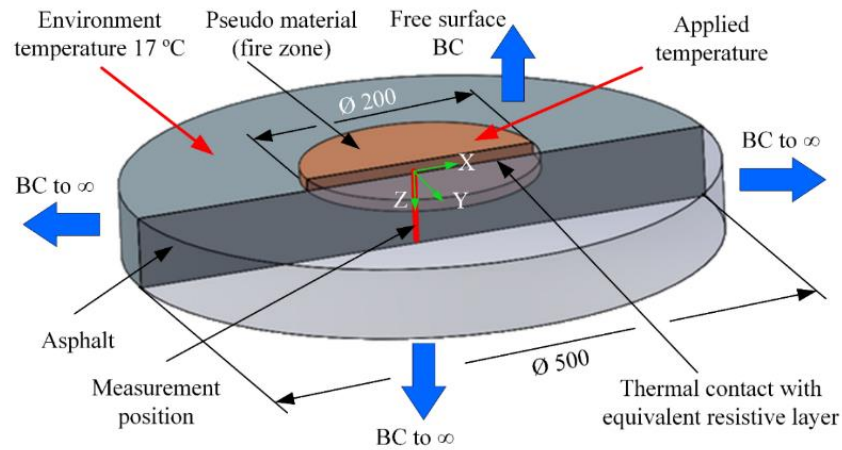


Figure 3. Boundary conditions (BC) of FEM model of asphalt fragment (here the red line is the center axis of the model and was used for the investigation of temperature distribution).

Table 2. This is a table. Tables should be placed in the main text near to the first time they are cited.

Model Parameters	Without Mechanical Impact	With Mechanical Impact 4500 N	Units
Initial temperature	17	17	°C
Coefficient of thermal expansion	10×10^{-6}	10×10^{-6}	1/K
Density	2700	3000	kg/m ³
Heat capacity at constant pressure	600	700	J/(kg K)
Heat transfer coefficient	32	32	W/(m ² ·K)
Layer conductance at thermal contact	100	100	W/(m ² ·K)
Poisson coefficient	0.4	0.4	-
Radiative conductance at thermal contact	500	100	W/(m ² ·K)
Surface emissivity	0.8	0.8	-
Thermal conductivity	2.7	3.5	W/(m·K)
Young 's modulus	40	40	GPa

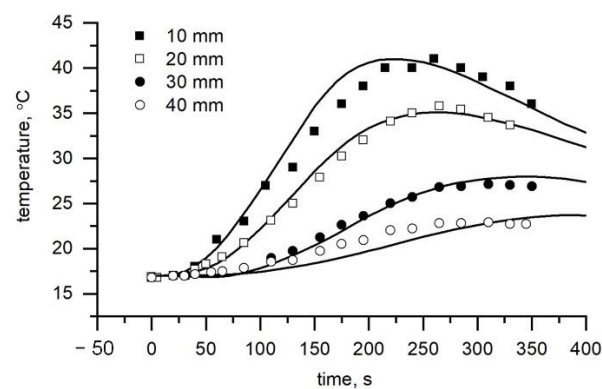


Figure 4. Temperature dependence on time, when the temperature of asphalt surface reached 250 °C (here the experimental data are represented by squares and round symbols, modeling results—by continuous lines).

3. Experiments

3.1. Experimental Setup

The experimental setup consists of a few main components (Figure 5a): a heating apparatus, a device for asphalt surface temperature measurement, and a measurement system for measuring the temperature of asphalt layers. For experimental tests, the heating apparatus AGRH-22 was used [28]. It is intended for heating asphalt in small area road construction; its total power is ~ 22 kW; the working temperature is $100\text{--}500$ °C. It can heat the surface area up to $800\text{ mm} \times 1170\text{ mm}$ and has 22 heating boards. The asphalt heater is equipped with a gas flow, automatic temperature regulators, and catalytic coating.

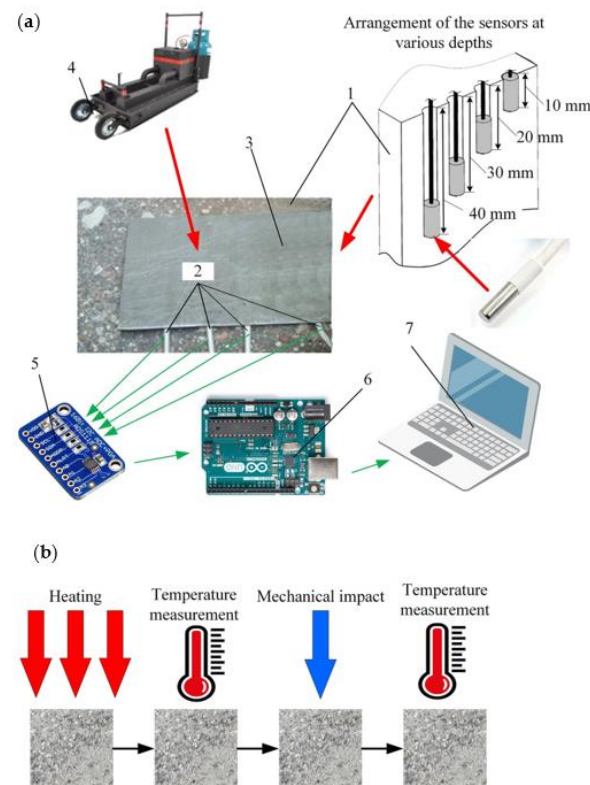


Figure 5. Scheme of the experiment: (a) setup (here 1—asphalt, 2—sensors, 3—protective plate, 4—heating apparatus, 5—analogue-digital converter, 6—microcontroller, 7—computer) and (b) procedure.

The asphalt surface temperature has been measured using a non-contact infrared thermometer GM320. It is based on measuring the strength of the emitted infrared spectrum with a measurement range of $-50\text{--}380$ °C ($-58\text{--}716$ °F).

The asphalt layer temperature has been measured using a specially designed system, based on the Arduino microcontroller and PT100-50/+500 °C temperature sensors. Sensors PT100 have $\text{Ø}3 \times 6$ mm size casing and can measure temperature in the range from 50 °C to 500 °C. These sensors have tolerance class B (0.2%), and their temperature coefficient is 3.85 nppm/°C. Silicone insulation has been used to protect the cable thermally. This insulator retains its properties up to 180 °C. Additionally, for the protection of wires from heat, heat-resistant glass fiber tubes (diameter of 6 mm) have been used. Such insulation provides thermal protection against temperatures of up to 400 °C.

Analog signal from sensors was converted into digital using the inline four-channel 16-bit analog-to-digital converter (ADC) ADS1115. It was connected to the Arduino Uno microcontroller, which was responsible for data acquisition, postprocessing, and transmission to the computer. The measurement system was adjusted to provide data every 20 s. Each data point transmitted to the computer was averaged from five consecutive measurements.

All data has been recorded using the PLX-DQ application, which allows saving data from a microcontroller to a Microsoft Excel worksheet data. This program application provides the possibility to save real-time data in Microsoft Excel and perform further processing.

3.2. Experimental Methodology

The experimental procedure started with the installation of temperature sensors. They were inserted into the drilled $\text{Ø}8$ mm holes at four depths: 10 mm, 20 mm, 30 mm, and 40 mm (Figure 5a). The spacing between the holes was selected at about 3–4 cm, considering the unevenness of the asphalt surface. The depth was selected because the asphalt layer could be cut up to 40 mm depth during the asphalt rehabilitation process [7]. To prevent sensors from direct heat and undistorted data through the existing drill gaps, the installation place was covered by a metal plate. During the experiment, the outdoor temperature was $20\text{ }^{\circ}\text{C}$ and the asphalt surface temperature was $17\text{ }^{\circ}\text{C}$.

The existing pavement stretch with asphalt wearing layer of asphalt concrete mixture type with the maximum particle size of 16 mm (AC 16 PD) was selected. Asphalt mixture binder type—100/150, bitumen content 5.2%, air void content—3%, aggregate type—gravel.

The experimental procedure is schematically described in Figure 5b. Firstly the asphalt was heated until the required surface temperature T_H ($250\text{ }^{\circ}\text{C}$, $300\text{ }^{\circ}\text{C}$, $350\text{ }^{\circ}\text{C}$, $400\text{ }^{\circ}\text{C}$, and $450\text{ }^{\circ}\text{C}$) was reached. After this, heating was continued for 3 min (180 s), measuring its temperature every 20 s. This allowed the heat to penetrate deeper layers of the asphalt. After that, the heated asphalt spot's central area ($20\text{ mm} \times 100\text{ mm}$) with installed sensors was loaded by a distributed mechanical force of 4500 N.

During each experiment, time-dependent temperature distribution characteristics showing temperature variation in every asphalt layer have been obtained. This makes it possible to evaluate the impact of mechanical treatment on the asphalt thermal conductivity.

4. Results and Discussions

4.1. Experimental Results

The asphalt layer was heated until surface temperature T_H reached $250\text{ }^{\circ}\text{C}$, $300\text{ }^{\circ}\text{C}$, $350\text{ }^{\circ}\text{C}$, $400\text{ }^{\circ}\text{C}$ or $450\text{ }^{\circ}\text{C}$ temperatures (Figure 6). By a visual assessment, the surface of the asphalt became darker as bituminous reached the melting temperature. The temperature of deeper layers was measured by sensors, placed in 10 mm, 20 mm, 30 mm, and 40 mm depth. The heating was stopped, and the mechanical load was applied at a moment, marked by a red line in Figure 6 till the end of the experiment. The temperature of all the measured layers increased after mechanical impact. It was also observed that after the 6th minute when applied heating was $250\text{ }^{\circ}\text{C}$ at 10 mm and 20 mm, the temperature started to decrease, whereas at 30 mm and 40 mm the temperature did not change (Figure 6a). At T_H $300\text{ }^{\circ}\text{C}$, the highest temperature change was observed at 10 mm (Figure 6b). The deformation of asphalt due to the melting at T_H $350\text{ }^{\circ}\text{C}$, $400\text{ }^{\circ}\text{C}$, or $450\text{ }^{\circ}\text{C}$, distorted the measured data (Figure 6c–e).

The summary of heating data is provided in Figure 7. When the heating temperature (T_H) of the surface reached $250\text{ }^{\circ}\text{C}$, the highest mechanical impact was at a depth of 20 mm, where the temperature difference was $6\text{ }^{\circ}\text{C}$: $T = 30\text{ }^{\circ}\text{C}$ and $T = 36\text{ }^{\circ}\text{C}$ before and after the applied load, respectively. The sensor, mounted at a depth of 10 mm, before the impact of the additional force, indicates a temperature of $102.49\text{ }^{\circ}\text{C}$. When the surface was heated to $T_H = 300\text{ }^{\circ}\text{C}$, at a depth of 10 mm, the temperature changed by $0.81\text{ }^{\circ}\text{C}$, at a depth of 20 mm the temperature changed by $1.71\text{ }^{\circ}\text{C}$, at a depth of 30 mm the temperature changed by $2.02\text{ }^{\circ}\text{C}$, and at a depth of 40 mm the temperature changed by $1.26\text{ }^{\circ}\text{C}$. These results showed that more heat penetrated deeper layers of the asphalt and a higher variation of temperature was in the middle (20–30 mm) layers.

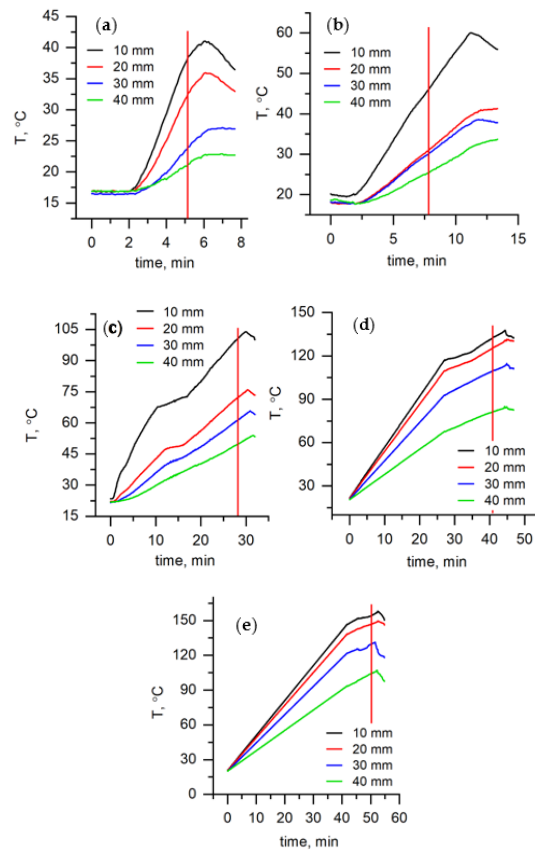


Figure 6. Temperature dependence on time at various depths when the temperature of the surface T_H reached: (a) 250 °C, (b) 300 °C, (c) 350 °C, (d) 400 °C, and (e) 450 °C.

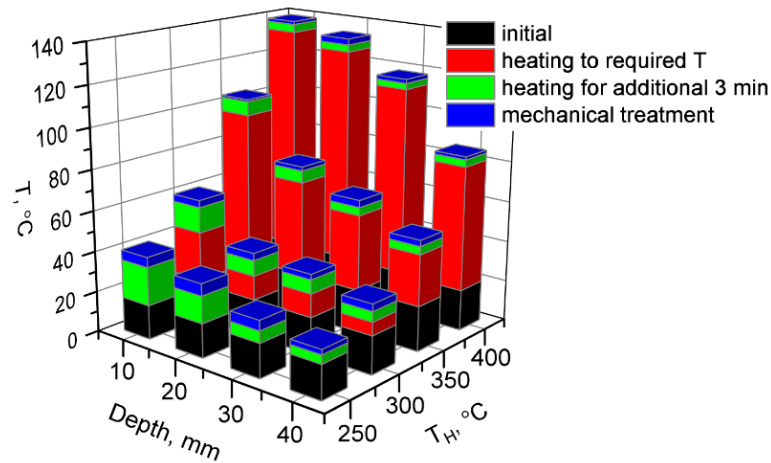


Figure 7. Summary of the heating data (here T_H —the temperature of the surface).

The experimental results have shown the effectiveness of the mechanical impact. After mechanical exposure, the temperature increased in all layers. After completion of the test, it was observed that the asphalt surface has become softer and slightly deformed due to the mechanical impact. The results show that heat transfer is relatively large.

4.2. Results from the Asphalt Layers Model

The distribution of temperature in the asphalt model has been simulated at different heating times (Figure 8). Heating stopped at 150 s; however, the highest temperature was

observed at 170 s (Figure 8d). At 250 s (Figure 8e), the upper layer becomes cooler, and heat distribution increases. The heating temperature is distributed in the deepest layers at 350 s.

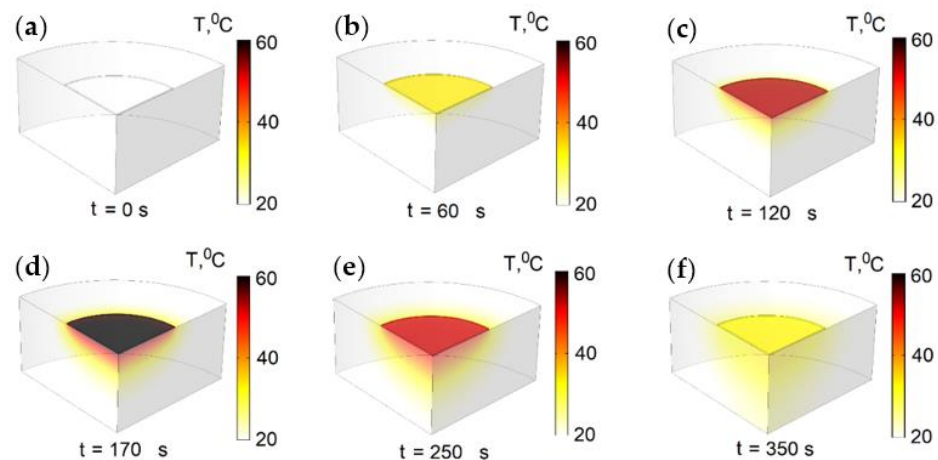


Figure 8. Distribution of temperature in asphalt model (the heated surface reached the temperature of 250 °C), (a) heating time 0 s, (b) heating time 60 s, (c) heating time 120 s, (d) heating time 170 s, (e) heating time 250 s, (f) heating time 350 s.

It was found that the temperature of the asphalt layers increased after a mechanical impact (Figure 9). A significant rise in temperature was observed in the deeper layers after the application of a mechanical impact. Since the asphalt was forced from the top, it was considered that this procedure increased the transfer of heat. The temperature increased significantly. However, the total amount of heat in the specimen remained constant. The theoretical study indicated that temperature variations between different layers were higher than by heating or by mechanical impact. The temperature increased in all layers after the mechanical loading.

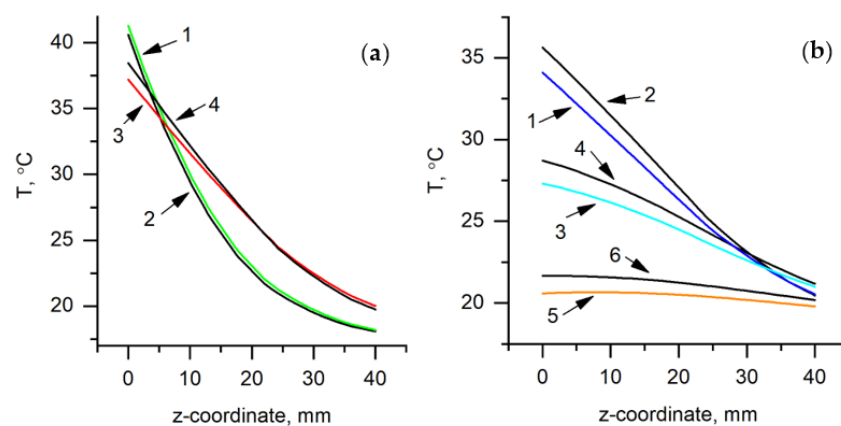


Figure 9. Temperature dependencies on z-coordinate with and without mechanical impact. (a) after 200 s and 300 s. 1—200 s, without mechanical impact; 2—200 s, with mechanical impact; 3—300 s, without mechanical impact; 4—300 s, with mechanical impact. (b) After 350 s, 500 s, 900 s. 1—350 s, without mechanical impact; 2—350 s, with mechanical impact; 3—500 s, without mechanical impact; 4—500 s, with mechanical impact; 5—900 s, without mechanical impact; 6—900 s, with mechanical impact.

5. Conclusions

The developed analytical model would allow selecting the regimes of the heating and mechanical deformation without conducting new experimental tests. It would also provide the required conditions for asphalt heating. The model would allow the selection

of heating and mechanical deformation modes without a new experimental test, as well as the determination of different asphalt heating rates. Asphalt was melted, and deformations were visible after the mechanical impact. However, after the mechanical impact, the rate of cooling varied significantly. It was assumed, that in order to transfer heat to lower layers, the top layer of the asphalt must reach a certain temperature so that the total amount of internal heat of the material is sufficient. It is adequate to raise the temperature of the deeper layers. If the surface temperature is too low, it is not sufficient to transfer heat to deeper layers.

The mechanical impact has a contribution to the heating transmission of the particle-binder-particle model, reducing the distance and increasing the contact points of particles in the asphalt mixture. However, the variation in temperature is quite limited as the results show. Meanwhile, the objective recycling temperature inside the asphalt layer can be obtained by increasing the heating time. In practice, how much the improvement in terms of heat transmission in the asphalt surface layer and how to implement the mechanical impact during the recycling process are unclear. Although the authors presented a possibility of improvement in heat transmission caused by mechanical impact, the effectiveness of this technique needs to be verified in the recycling site.

Author Contributions: Conceptualization, V.B. and A.D.; methodology, V.B. and A.D.; software, A.D. and I.M.-V.; validation, A.D., M.M. and I.M.-V.; investigation, V.B., A.D., M.M. and N.S.; resources, V.B.; data curation, M.M.; writing—original draft preparation, V.B., A.D., N.S., M.M. and I.M.-V.; writing—review and editing, V.B., A.D., N.S., M.M. and I.M.-V.; visualization, A.D.; supervision, V.B.; funding acquisition, V.B. All authors have read and agreed to the published version of the manuscript.

Funding: This work is part of the AI4SCM project, receiving funding from the European H2020 research and innovation programme, ECSEL Joint Undertaking, under grant agreement No.101007326.

Institutional Review Board Statement: Not applicable.

Informed Consent Statement: Not applicable.

Data Availability Statement: Not applicable.

Conflicts of Interest: The authors declare no conflict of interest.

References

1. Tauste, R.; Moreno-Navarro, F.; Sol-Sánchez, M.; Rubio-Gámez, M.C. Understanding the Bitumen Ageing Phenomenon: A Review. *Constr. Build. Mater.* **2018**, *192*, 593–609. [[CrossRef](#)]
2. Pereira, P.; Pais, J. Main Flexible Pavement and Mix Design Methods in Europe and Challenges for the Development of an European Method. *J. Traffic Transp. Eng. (Engl. Ed.)* **2017**, *4*, 316–346. [[CrossRef](#)]
3. Moreno-Navarro, F.; Sol-Sánchez, M.; García-Travé, G.; Rubio-Gámez, M.C. Fatigue Cracking in Asphalt Mixtures: The Effects of Ageing and Temperature. *Road Mater. Pavement Des.* **2018**, *19*, 561–570. [[CrossRef](#)]
4. Yu, H.; Bai, X.; Qian, G.; Wei, H.; Gong, X.; Jin, J.; Li, Z. Impact of Ultraviolet Radiation on the Aging Properties of SBS-Modified Asphalt Binders. *Polymers* **2019**, *11*, 1111. [[CrossRef](#)]
5. Zeng, W.; Wu, S.; Pang, L.; Chen, H.; Hu, J.; Sun, Y.; Chen, Z. Research on Ultra Violet (UV) Aging Depth of Asphalts. *Constr. Build. Mater.* **2018**, *160*, 620–627. [[CrossRef](#)]
6. Kleiziene, R.; Panasienkiene, M.; Vaitkus, A. Effect of Aging on Chemical Composition and Rheological Properties of Neat and Modified Bitumen. *Materials* **2019**, *12*, 4066. [[CrossRef](#)]
7. Xiao, F.; Yao, S.; Wang, J.; Li, X.; Amirkhanian, S. A Literature Review on Cold Recycling Technology of Asphalt Pavement. *Constr. Build. Mater.* **2018**, *180*, 579–604. [[CrossRef](#)]
8. Liu, Y.; Wang, H.; Tighe, S.L.; Zhao, G.; You, Z. Effects of Preheating Conditions on Performance and Workability of Hot In-Place Recycled Asphalt Mixtures. *Constr. Build. Mater.* **2019**, *226*, 288–298. [[CrossRef](#)]
9. Xu, X.; Gu, H.; Dong, Q.; Li, J.; Jiao, S.; Ren, J. Quick Heating Method of Asphalt Pavement in Hot In-Place Recycling. *Constr. Build. Mater.* **2018**, *178*, 211–218. [[CrossRef](#)]
10. Li, J.; Ni, F.; Huang, Y.; Gao, L. New Additive for Use in Hot In-Place Recycling to Improve Performance of Reclaimed Asphalt Pavement Mix. *Transp. Res. Rec.* **2014**, *2445*, 39–46. [[CrossRef](#)]
11. Vaitkus, A.; Gražulytė, J.; Baltrušaitis, A.; Židanavičiūtė, J.; Čygas, D. Long-Term Performance of Pavement Structures with Cold in-Place Recycled Base Course. *Baltic J. Road Bridge Eng.* **2021**, *16*, 48–65. [[CrossRef](#)]
12. Cao, R.; Leng, Z.; Hsu, M.S.-C. Eco-Efficiency Analysis on Asphalt Pavement Rehabilitation Alternatives: Hot In-Place Recycling (HIPR) and Milling and Filling (M&F). *Destech Trans. Eng. Technol. Res.* **2017**, 56–63. [[CrossRef](#)]

13. Zaumanis, M.; Mallick, R.B.; Frank, R. 100% Hot Mix Asphalt Recycling: Challenges and Benefits. *Transp. Res. Procedia* **2016**, *14*, 3493–3502. [[CrossRef](#)]
14. Yu, B.; Wang, S.; Gu, X.; Ni, F.; Liu, Q. Environmental Burden Evaluation of Hot In-Place Recycling of Asphalt Pavement Based on Discrete Event Simulation. *Transp. Res. D Transp. Environ.* **2018**, *65*, 151–160. [[CrossRef](#)]
15. Huang, K.; Xu, T.; Li, G.; Jiang, R. Heating Effects of Asphalt Pavement during Hot In-Place Recycling Using DEM. *Constr. Build. Mater.* **2016**, *115*, 62–69. [[CrossRef](#)]
16. Al-Bayati, H.K.A.; Tighe, S.L.; Achebe, J. Influence of Recycled Concrete Aggregate on Volumetric Properties of Hot Mix Asphalt. *Resour. Conserv. Recycl.* **2018**, *130*, 200–214. [[CrossRef](#)]
17. Kaseer, F.; Martin, A.E.; Arámbula-Mercado, E. Use of Recycling Agents in Asphalt Mixtures with High Recycled Materials Contents in the United States: A Literature Review. *Constr. Build. Mater.* **2019**, *211*, 974–987. [[CrossRef](#)]
18. Zaumanis, M.; Mallick, R.B.; Frank, R. 100% Recycled Hot Mix Asphalt: A Review and Analysis. *Resour. Conserv. Recycl.* **2014**, *92*, 230–245. [[CrossRef](#)]
19. Erlingsson, S. Modelling of Rutting Development in Pavement Structures. *Procedia Soc. Behav. Sci.* **2012**, *48*, 321–330. [[CrossRef](#)]
20. Pan, P.; Wu, S.; Hu, X.; Liu, G.; Li, B. Effect of Material Composition and Environmental Condition on Thermal Characteristics of Conductive Asphalt Concrete. *Materials* **2017**, *10*, 218. [[CrossRef](#)]
21. Table A1 Thermal Conductivity of Some Common Building Materials | The Irish Building Regulations Technical Guidance Documents—Home. Available online: <https://www.housebuild.com/construction/building-regulations/building-regulations-and-other-guidance/part-1-2019/appendix-a-calculations-of-u-values> (accessed on 20 November 2021).
22. Emmanuel, S.; Eliyahu, M.; Day-Stirrat, R.J.; Hofmann, R.; Macaulay, C.I. Softening of Organic Matter in Shales at Reservoir Temperatures. *Pet. Geosci.* **2017**, *23*, 262–269. [[CrossRef](#)]
23. Zhu, X.Y.; Chen, L. Numerical Prediction of Elastic Modulus of Asphalt Concrete with Imperfect Bonding. *Constr. Build. Mater.* **2012**, *35*, 45–51. [[CrossRef](#)]
24. Vikhrenko, V.S. *Heat Transfer—Engineering Applications*; InTech: Vienna, Austria, 2012.
25. Tariku, F.; Kumaran, K.; Fazio, P. Transient Model for Coupled Heat, Air and Moisture Transfer through Multilayered Porous Media. *Int. J. Heat Mass Transf.* **2010**, *53*, 3035–3044. [[CrossRef](#)]
26. COMSOL Multiphysics Heat Transfer Module. Manual 2015. pp. 1–222. Available online: <https://doc.comsol.com/5.4/doc/com.comsol.help.heat/HeatTransferModuleUsersGuide.pdf> (accessed on 21 September 2021).
27. T'ien, J.S. Principles of Combustion. *Combust. Flame* **1988**, *73*, 337. [[CrossRef](#)]
28. Gas Radiant Heaters. Available online: <http://gasradiantheaters.eu/portable-infrared-asphalt-heaters/> (accessed on 9 April 2020).